Hydrogen Effect on Dislocation Emission from a Crack Tip in Alpha Iron

S. Taketomi[1], R. Matsumoto[1], S. Matsumoto[2], N. Miyazaki[1]
[1]*Kyoto University, Kyoto, Japan;* [2]*Graduate School of Engineering, Kyoto University, Kyoto, Japan*

1 Introduction

Hydrogen embrittlement is one of the issue should be clarified for the safe usage of hydrogen storage components. According to the experimental fact that hydrogen significantly decreases the ductility of steel[1], it is believed that hydrogen embrittlement fracture is responsible for the feature of dislocation motion. Interaction between dislocations in the presence of hydrogen has been extensively investigated by many researchers[2,3]. Note that, the effect of hydrogen on dislocation emission is also important for the understanding of mechanical properties of metal. It is experimentally recognized that hydrogen enhances the dislocation emission[4-7], however the exact reason for this phenomenon has not been well clarified. Decrement of the cohesive energy[5,6] or decrement of the elastic modulus[6,7] are reported to attribute the enhancement of the dislocation emission.

On the other hand, J. R. Rice conducted a theoretical study[8] for the dislocation emission from a crack tip based on Peierls model. And he proposed an equation which represents the relationship between the critical stress intensity factor for dislocation emission and the material constants (stacking fault energy, Poisson's ratio and shear modulus). This equation enables us to estimate which parameter (stacking fault energy or shear modulus) could be effective for dislocation emission in the presence of hydrogen.

In this study, molecular statics analysis based on atomistic model is performed, and the effect of hydrogen on critical stress intensity factor for dislocation emission from a crack tip is investigated. Moreover, obtained stress intensity factor is compared with theoretical expression proposed by Rice. In his calculation, thermal fluctuation term is not taken into account. Therefore molecular statics is adopted in this study. The material which used in this study is bcc structured alpha iron because pure iron is also reported to be sensitive to hydrogen[9,10] and its alloys are expected to serve as hydrogen storage and piping components due to their low cost.

2. Analysis method

The analysis model in this study is shown in Fig. 1. A cylindrical disk with radius R = 8.9 nm and thickness B = 2.0 nm is prepared as an analysis model. In order to introduce a mode II initial crack into the system, iron atoms within 3.0 nm length

and 0.4 nm width along the x axis from the outer edge are removed as shown in Fig.1. {112} slip plane is arranged along the crack plane to generate an edge dislocation from the crack tip under mode II stress condition. The number of iron atom is approximately 43000, and periodic boundary condition is adopted along z direction. In this study, embedded atom method(EAM) potential developed by Wen et al.[11] is adopted as an interatomic potential which expresses the atomistic interactions.

The atoms within 0.7 nm from the cylinder surface as shown in Fig.1(shaded region) are the boundary atoms. In order to estimate the critical stress intensity factor(K_{IIc}) for dislocation emission, the boundary atoms are forced to displace based on the linear elastic solution of displacement around mode II crack. The displacement is given as following equation (1).

$$\begin{Bmatrix}\Delta u\\ \Delta v\end{Bmatrix} = -\frac{\Delta K_{\mathrm{II}}}{2G}\sqrt{\frac{r}{2\pi}}\begin{Bmatrix}\sin\dfrac{\theta}{2}\left(\kappa+1+2\cos^2\dfrac{\theta}{2}\right)\\ -\cos\dfrac{\theta}{2}\left(\kappa-1-2\sin^2\dfrac{\theta}{2}\right)\end{Bmatrix}, \tag{1}$$

where, Δu and Δv are the increment of displacement along x and y directions respectively. ΔK_{II} is the increment of stress intensity factor, G is the shear modulus, r is the distance from the crack tip and θ is the degree from the crack plane. Here, the analysis model satisfies the plane strain condition. Therefore, $\kappa = 3 - 4\nu$, where ν is the Poisson's ratio. In this analysis, boundary atoms are given constrained displacements with $\Delta K_{\mathrm{II}} = 1.5 \times 10^{-3}$ MPam$^{1/2}$ for every steps, then the conjugate gradient(CG) method is adopted to relax the positions of the other atoms. During the relaxation process the boundary atoms are fixed within the xy plane. These treatments are performed for 400 steps until the stress intensity factor K_{II} reaches 0.6 MPam$^{1/2}$.

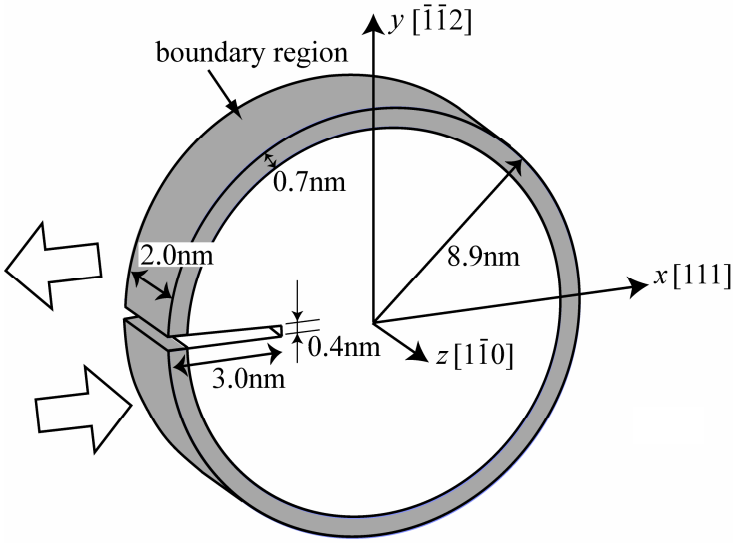

Fig.1 Geometry and crystalline orientations of the analysis model.

3. Results and discussion

3.1 Stress intensity factor for dislocation emission in the absence of hydrogen

The critical stress intensity factor for dislocation emission from the crack tip is investigated in the absence of hydrogen. The boundary atoms are given constrained displacement with the distance of respective stress intensity factor. Here the relationship between the total potential energy of the system and the applied stress intensity factor during the calculation is shown in Fig.2. As the applied stress intensity factor K_{II} increases, the total potential energy of the system increases gradually. When the stress intensity factor reaches the critical value, the total energy of the system decrease with an edge dislocation emission as shown in Fig.2 (a) and (b). In these figures, green spheres are the non-bcc structured atoms. The crystalline structures are estimated using CNA(Common Neighbor Analysis) method. Thus the critical value of stress intensity factor for dislocation emission from the crack tip is evaluated as K_{IIc} = 0.443 MPam$^{1/2}$. In this analysis, the K_{II} is summed up with the discrete values, hence the accuracy is guarantied with the $\Delta K_{II} = + 1.5 \times 10^{-3}$ MPam$^{1/2}$. Critical value of stress intensity factor for dislocation emission in nature is supposed to be rather small (i.e. three-dimensional dislocation loop emission, thermal fluctuation). This molecular statics result reveals athermal condition for leading dislocation emission.

Rice theoretically proposed the critical stress intensity factor for edge dislocation emission along the crack plane from the mode II crack tip as the following equation.

$$K_{IIc} = \sqrt{\frac{2G_{slip}\gamma_{us}}{1-\nu}} \quad , \tag{2}$$

where, G_{slip} is the shear modulus, γ_{us} is the stacking fault energy, ν is the Poisson's ratio. Shear modulus along the slip plane in cubic materials is written as $G_{slip} = (C_{11}-C_{12}+C_{44})/3$ [8], here C_{11} = 228.0 GPa, C_{12} = 134.6 GPa and C_{44} = 112.0 GPa for alpha iron. Thus, G_{slip} = 68.5 GPa can be obtained. Stacking fault energy for {112}<111> is calculated as 1.03 J/m^2 in the absence of hydrogen. Poisson's ratio is assumed using the Voigt average concept, ν = 0.28. Substituting these values to the equation (2), K_{IIc} = 0.489 MPam$^{1/2}$ can be obtained. This theoretical result is in good agreement with our molecular statics result with an error of 9.6% (K_{IIc} = 0.443 MPam$^{1/2}$).

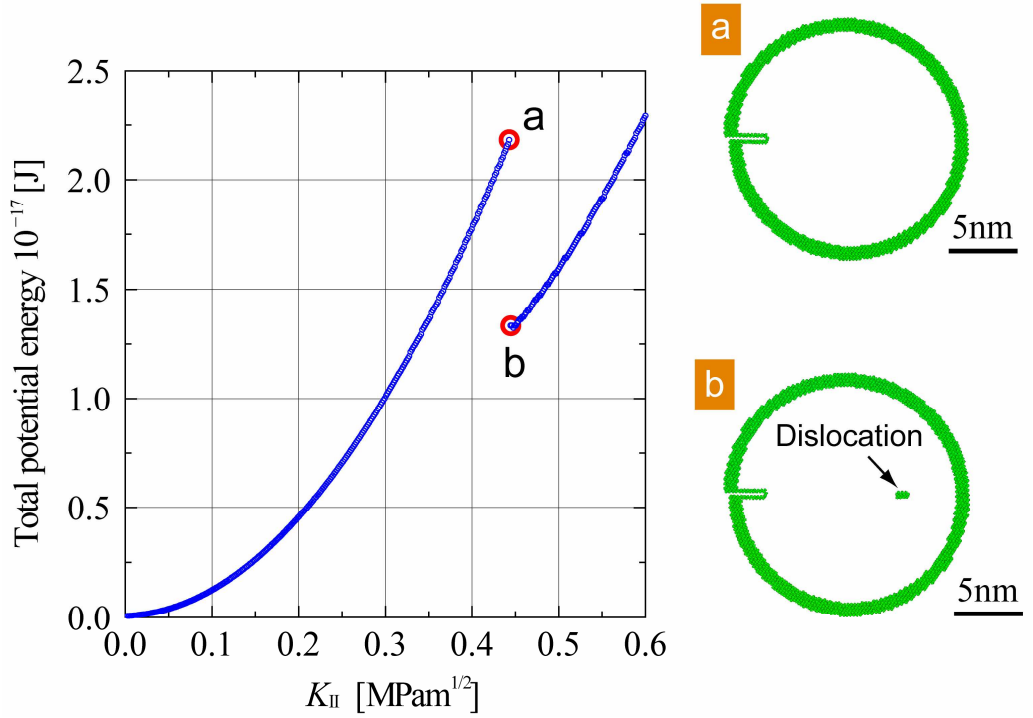

Fig.2 Sequential of the total potential energy of the system during the deformation. The crystalline structure is estimated using Common Neighbor Analysis (CNA) for both (a) and (b). Non-bcc structured atoms are colored by green in (a) and (b). An edge dislocation is emitted from the crack tip at the critical stress intensity factor.

3.2 Hydrogen-trap energy distribution around a mode II crack tip

In order to estimate the hydrogen position around a stressed crack tip in nature, hydrogen-trap energy distribution around a crack tip is investigated. The calculation method of hydrogen-trap energy is the same as our previous study[12]. Initially, hydrogen atom is introduced into the entire T and O sites around the crack tip which estimated by Voronoi tessellation. Then the atomistic structures are relaxed to minimize the total energy of the system. Hydrogen-trap energy at each occupation site is given as follows.

$$\Delta E_d(\boldsymbol{r}) = -\left[\Phi_{\mathrm{Fe+H}}(\boldsymbol{r}) - \left\{\Phi_{\mathrm{Fe}} - \frac{1}{2}E_b + E_s\right\}\right], \qquad (3)$$

where, $\Phi_{\mathrm{Fe+H}}(\boldsymbol{r})$ is the total potential energy of the system with hydrogen atom at $\boldsymbol{r}$ trap site, Φ_{Fe} is the total potential energy of the system in the absence of hydrogen, E_b is the binding energy of the hydrogen molecules, E_s is the heat of solution to the T site. Hydrogen-trap energy distribution around a crack tip is shown in Fig.3. Here the applied stress intensity factor ΔK for boundary atoms is 0.4 MPam$^{1/2}$.

Hydrogen-trap energies are strong at the upper side of the crack due to high hydrostatic stress, in contrast, the hydrogen-trap energies are weak at the lower side of the crack. According to our previous study[12], hydrogen-trap energy has

the dependence not only hydrostatic stress but also shear stress in this crystalline orientation. Hydrogen-trap energy is also strong at the vicinity of crack tip front, where hydrostatic stress is low but shear stress is high. These results indicate that hydrogen-trap energy is affected both hydrostatic stress and shear stress around the crack tip. Here, the hydrogen-trap energies at these trap sites are sufficiently strong to trap a hydrogen atom at room temperature.

3.3 Effect of hydrogen on dislocation emission

Distribution of critical stress intensity factor for dislocation emission at each hydrogen occupation site is shown in Fig.4. The minimum stress intensity factor for dislocation emission is $K_{\mathrm{IIc}} = 0.402$ MPam$^{1/2}$ at the vicinity of the crack tip region(occupation site (a) in Fig.4). Increasing the distance from crack tip, critical stress intensity factor increases significantly. Hence, effective region of hydrogen atom for dislocation emission is limited within a few angstroms from a crack tip. Since hydrogen atom stably exists near the crack tip as shown in Fig.3, it is assumed that hydrogen atom contributes dislocation emission at lower stress level.

Effects of hydrogen on material constants are investigated. The relation of shear modulus and Poisson's ratio with hydrogen concentration for unit volume are shown in Fig.5. The relation with stacking fault energy and hydrogen concentration for unit area is shown in Fig.6. Shear modulus and Poisson's ratio converge to the values when the hydrogen concentration takes over 2 nm^{-3}. Stacking fault energy, however, lineally decreases in increasing the hydrogen concentration. The theoretical prediction proposed by Rice is in good agreement with our atomistic simulation results, therefore the reduction of stacking fault energy is considered to be the main reason for the enhancement of dislocation emission.

When a hydrogen atom positioned at 0.4 nm from a crack tip (position (a) in Fig.4), the hydrogen concentration is approximately 1.25 nm^{-2}. According to the relationship between stacking fault energy and hydrogen concentration as shown in Fig.5, 8.79% decrement of stacking fault energy occurs. Due to the equation (2), critical stress intensity factor decreases 4.50% ($K_{\mathrm{IIc}} = 0.467$ MPam$^{1/2}$). This decrement is quantitatively in good agreement with the results shown in Fig.4 ($K_{\mathrm{IIc}} = 0.402$ MPam$^{1/2}$ at the hydrogen occupation site (a)).

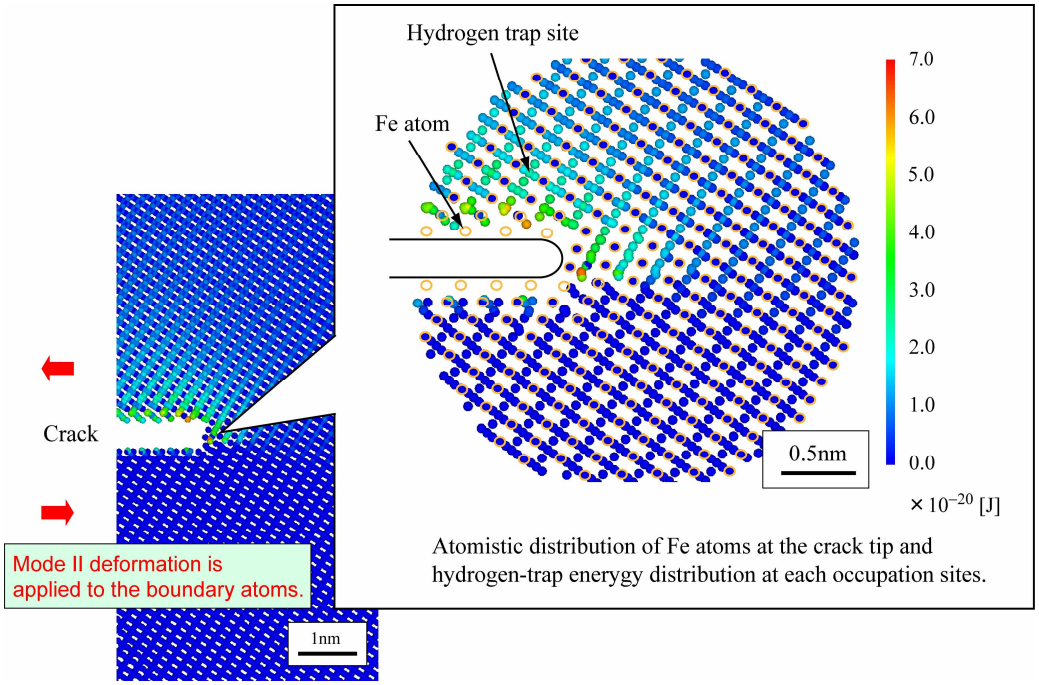

Fig.3 Hydrogen-trap energy distribution around a mode II crack tip for each occupation sites. Left: hydrogen-trap energies at each occupation sites. Right: Fe atoms are illustrated in orange circles and other spheres are hydrogen trap sites. Here the applied stress intensity factor ΔK for boundary atoms is 0.4 MPam$^{1/2}$.

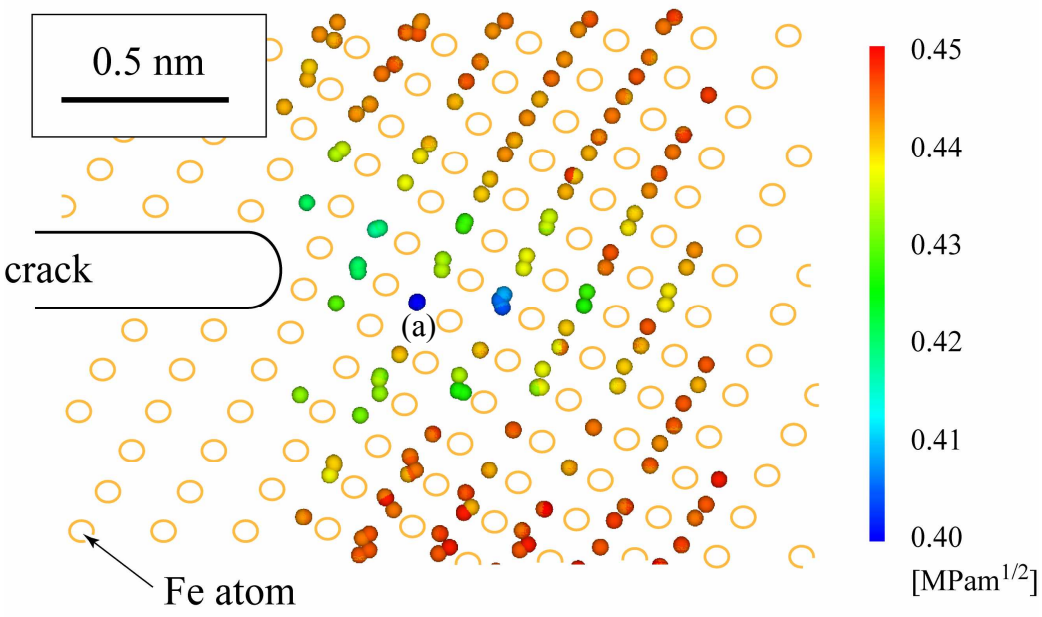

Fig.4 Distribution of critical stress intensity factor for dislocation emission at each hydrogen occupation site

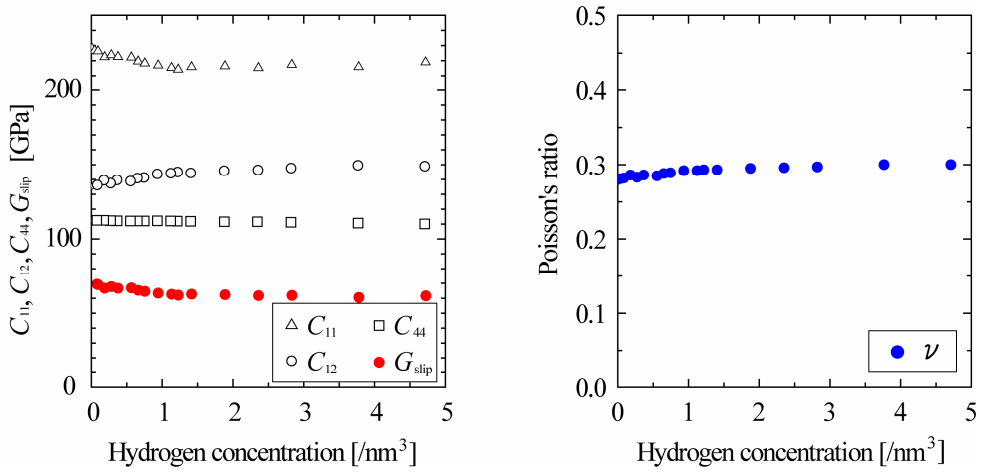

Fig.5 Relationship of hydrogen concentration with elastic modulus and Poisson's ratio.

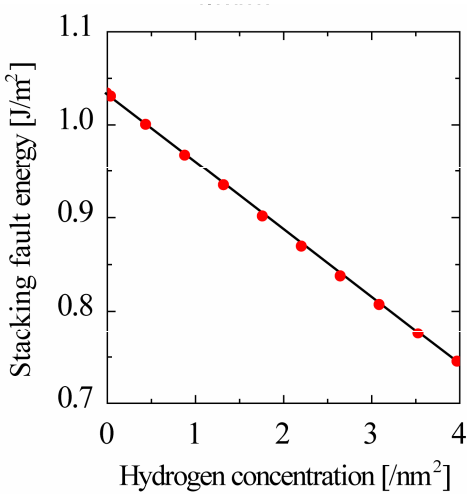

Fig.6. Relationship between hydrogen concentration and stacking fault energy.

4 Conclusions

We investigated the effect of hydrogen on {112}<111> edge dislocation emission from a mode II crack tip in alpha iron based on atomistic model. And the following conclusions are obtained.

1. A hydrogen atom around a crack tip enhances the dislocation emission around a crack tip. Note that, the effective distance of hydrogen atom for dislocation emission is limited within a few angstroms from a crack tip.

2. Decrement of critical stress intensity factor for dislocation emission in the presence of hydrogen is thought to be attributed to the decrement of stacking fault energy.

References

[1] G. Han, J. He, S. Fukuyama, K. Yokogawa., Effect of strain-induced martensite on hydrogen embrittlement of sensitized austenitic steels at low temperatures, Acta Materialia 46 (1998) 4559-4570

[2] P. Sofronis, H. K. Birnbaum, Mechanics of the hydrogen-dislocation-impurity interactios -1. Increasing shear modulus, Journal of the Mechanics and Physics of Solids 43 (1) (1995) 49-90

[3] P. J. Ferreira, I.M.Robertson, H. K. Birnbaum, Hydrogen effects on the interaction between dislocations, Acta Materialia 46 (5) (1998) 1749-1757

[4] I. M. Robertson, H. K. Birnbaum, An HVEM study of hydrogen effects on the deformation and fracture of nickel, Acta Metallurgica 34 (3) (1986) 353-366

[5] J. A. Clum, The role of hydrogen in dislocation generation in iron alloys, Scripta Metallurgica 9 (1975) 51-58

[6] G. H. Zhou, F. X. Zhou, F. R. Wan, W. Y. Chu, Molecular dynamics simulation of hydrogen enhancing dislocation emission, Key Engineering Materials 145-149 (1998) 123-128

[7] K. A. Nibur, D. F. Bahr, B. P. Somerday, Hydrogen effects on dislocation activity in austenitic stainless steel, Acta Materialia 54 10 (2006) 2677-2684

[8] J. R. Rice, Dislocation nucleation from a crack tip: an analysis based on the peierls concept, Journal of Mechanics and Physics of Solids 40 (2) (1992) 239-271

[9] H. Matsui, H. Kimura, S. Moriya, The effect of hydrogen on the mechanical properties of high purity iron I. Softening and hardening of high purity iron by hydrogen charging during tensile deformation, Materials Science and Engineering 40 (1979) 207-216

[10] A. Kimura, H. Matsui, H. Kimura, The work-hardening behaviour of hydrogen-charged high purity iron single crystals at temperatures between 296 and 200K, Material Science and Engineering 58 (1983) 211-222

[11] M. Wen, X. J. Xu, S. Fukuyama, K. Yokogawa, Embedded-atom-method functions for the body-centered-cubic iron and hydrogen, Journal of Materials Research 16 (12) (2001) 3496-3502

[12] S. Taketomi, R. Matsumoto, N. Miyazaki, Atomistic study of hydrogen distribution and diffusion around a {112}<111> edge dislocation in alpha iron, Acta Materialia 56 (15) (2008) 3761-3769